Short-Range Exciton Couplings in LH2 Photosynthetic Antenna Proteins Studied by High Hydrostatic Pressure Absorption Spectroscopy

Kõu Timpmann,[†] Aleksandr Ellervee,[†] Tõnu Pullerits,[‡] Rein Ruus,[†] Villy Sundström,[‡] and Arvi Freiberg*,[†]

Institute of Physics, University of Tartu, Riia 142, 51014 Tartu, Estonia, and Department of Chemical Physics, Lund University, P.O. Box 124, S-22100 Lund, Sweden

Received: September 27, 2000; In Final Form: February 14, 2001

The effects of high hydrostatic pressure (up to 8 kbar) on bacteriochlorophyll *a* Q_y electronic absorption bands of LH2 photosynthetic antenna complexes have been studied at ambient temperature. A variety of samples were studied, including intact membranes and isolated complexes from wild type and mutant photosynthetic bacteria *Rhodobacter sphaeroides*, *Rhodopseudomonas acidophila*, and *Rhodospirillum molischianum*. The spectra of the complexes universally red shift and broaden under elastic compression, while the variations of the integrated intensity remain within the experimental uncertainty. A qualitatively different slope and variation of the slope of the pressure-induced shift is observed for the B800 and B850 absorption bands of LH2 complexes belonging to quasi-monomer and aggregated pigments, respectively. For the complexes from *Rhodobacter sphaeroides*, e.g., the corresponding slopes are -28 ± 2 and -65 ± 2 cm^{-1}/kbar. The shift rate of the B800 band declines with pressure, while the opposite is observed for the B850 band. The shifts show little if any correlation with hydrogen bonds. Using simple phenomenological arguments and numerical simulations of molecular exciton spectra, it is shown that the shift of the B800 band is governed by pigment−protein interactions, while in addition to that, interpigment couplings (including long-range dipolar and short-range orbital overlap interactions) are instrumental for the B850 band shift. The compressibility of the B800 bacteriochlorophyll binding sites deduced from the B800 band shift at ambient pressure is $\sim$0.02 $kbar^{-1}$, and it decreases nonlinearly with pressure. Inter-pigment couplings are responsible for approximately one-third of both the total ambient-pressure solvent shift of the B850 absorption band and its pressure-induced growth. A slight increase with pressure of the B850 band shift due to orbital overlap couplings is predicted.

Introduction

The optical properties of molecular systems depend on intermolecular interactions sensitive to distances and relative orientations of the coupled molecules. The main objective of this work is to study the character of the couplings between the bacteriochlorophyll *a* (Bchl) chromophores in peripheral (LH2) antenna protein complexes of purple photosynthetic bacteria using hydrostatic compression of the sample.

The lowest, Q_y, molecular electronic transition-related absorption band in the LH2 antenna complex has been shown to have a substantial exciton character.[1−6] In the absence of a direct orbital overlap, the resonant interaction between the chromophores causing the excitation transfer is mediated by a Coulomb interaction between the electronic transition densities of the molecules. In the multipolar expansion of the interaction potential usually only the dipole−dipole term is retained, giving a familiar R^{-3} distance dependence of the interaction energy. This approximation is valid at distances large compared to the molecular size, which is evidently not the case in the LH2 protein complexes where the closest approach between the Bchl molecules (having a core diameter $\sim$0.9 nm) is $\sim$0.35 nm[7,8] (see Figure 1). Under these circumstances, not only may the dipole−dipole approximation fail but also the electron density distributions of the adjacent Bchl molecules may overlap,[9−11] causing substantial deviations from the standard exciton model. Charge-transfer configurations have been found to play a central role in promoting orbital overlap dependent interactions. The expected distance dependence of those interactions is $\exp(-\gamma R)$, where γ is the decay constant that describes the attenuation of the coupling with distance, R.[9,11]

The dipolar approximation as a well-established theoretical approach has been routinely applied to interpret exciton spectra in molecular crystals of aromatic series, such as anthracene and tetracene.[1,2] And yet, the pressure experiments on the same series of crystals have shown that the factor group or Davydov splitting increases much stronger than expected based on not only dipolar but also multipolar terms of expansion of resonant interactions.[12−15] This has been taken as an indication of a short-range character of the intermolecular couplings. Here, we shall take a similar approach to test the electronic coupling mechanisms in the LH2 antenna protein complexes by studying their spectra under compression.

Precise tuning of the absorption properties of antenna protein complexes seems to be involved both in the funneling of exciton energy toward the reaction center (RC) protein complex[16−19] and in the adaptation of some of these photosynthetic organisms to varying environmental conditions.[20] Two near-infrared bands at about 800 and 850 nm characterize the absorption spectra of

* Corresponding author. Tel.: +3727383024. Fax: +3727383033. E-mail: freiberg@fi.tartu.ee.
[†] University of Tartu.
[‡] Lund University.

10.1021/jp003496f CCC: $20.00
Published on Web 08/10/2001

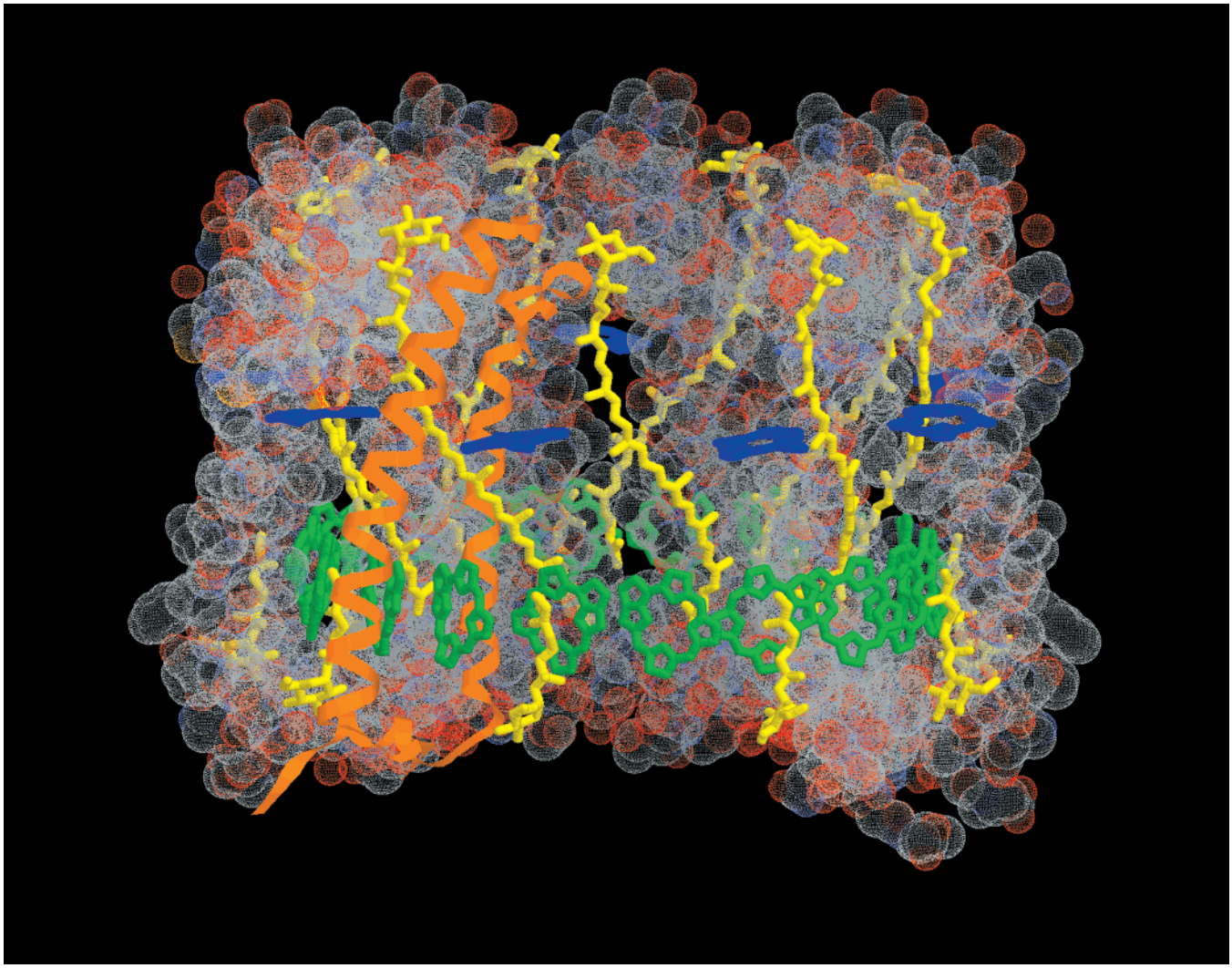

Figure 1. Structure of the LH2 antenna from *Rhodopseudomonas acidophila*.[7] The LH2 complex is composed of nine repetitions of a basic unit containing two membrane-spanning polypeptides (α and *β*, comprising 45−60 amino acid residues each), three noncovalently bound Bchl, and a carotenoid pigment. The 18 Bchl molecules forming a continuous overlapping ring of C_9 symmetry are located between the inner and the outer cylinders of polypeptides. These molecules (customarily labeled as B850) absorb light at 850 nm. The 9 Bchls located toward the cytoplasmic surface of the membrane (B800) are responsible for the absorption band at 800 nm. The carotenoid molecules make close contact simultaneously with the B850 and B800 chromophores. For clarity, only the porphyrin macrocycles of the Bchl pigments are shown.

aggregated Bchls in the LH2 antenna, while monomeric Bchl molecules absorb in most solvents at about 773 nm. It is now generally accepted that two different types of mechanisms underlie the apparent downshift of the absorption frequency of aggregated Bchl molecules in the antenna proteins compared to the monomer spectra, namely pigment−pigment interactions as well as pigment−protein couplings. Protein engineering, which allows manipulating protein residues near particular pigments, in combination with different types of spectroscopy, has proven to be very successful in uncovering the essence of the pigment−protein couplings. They involve hydrogen bonding between the protein and carbonyl groups of the Bchls, axial ligation (coordination of the central Mg atom of the Bchl molecule), and the influence of the polarizability in the vicinity of the carbonyl groups.[21−24] In contrast, pigment−pigment interactions have been less well characterized. These latter interactions are the main focus of the present work.

High-pressure tuning of absorption and fluorescence emission spectra of LH2 (as well as of LH1) antenna complexes over a wide spectral range and in a controlled manner was demonstrated both at ambient temperature and at cryogenic temperatures.[25−29] These studies have shown that increasing the pressure causes a substantial red shift and broadening of the Q_y absorption bands. The most appealing feature of the pressure dependence of the absorption spectrum of the LH2 antenna proteins is the disparity in the rate of shifts of the B800 and B850 absorption bands, first observed in ref 26. Based on the low-temperature measurements, this difference was assigned to the strong dipolar exciton coupling between the B850 pigments absent between the more loosely packed B800 molecules.[30]

In the present work, we study the effects of high hydrostatic pressures on the absorption spectra of LH2 antenna proteins. Pressures up to 8 kbar were applied at room, i.e., at physiological, temperature. As listed in Table 1, various sample solutions containing membrane-bound or detergent-isolated LH2 antenna protein complexes from three different purple non-sulfur photosynthetic bacterial species (*Rhodopseudomonas (Rps.) acidophila*, *Rhodospirillum (Rs.) molischianum*, and *Rhodobacter* (*Rb.*) *sphaeroides*) were investigated. Two spectrally different LH2 complexes develop in *Rps. acidophila* depending on the growth conditions. Here, we have studied in the solvent phase both regular B800−850 antenna complexes from the high light strain 10050 and the B800−820 complexes with strongly blue shifted redmost absorption band from the low light strain

TABLE 1: Pressure Shifts of the Q_y Absorption Bands of LH2 Antenna Complexes at Room Temperature[a]

	B800			B850/B820		
sample	A, cm^{-1}	S, cm^{-1} $kbar^{-1}$	C, cm^{-1} $kbar^{-2}$	A, cm^{-1}	S, cm^{-1} $kbar^{-1}$	C, cm^{-1} $kbar^{-2}$
Rps. acidophila, 10050[b]	12497.9 ± 2.6	-16.6 ± 2.4	0.3 ± 0.4	11640.1 ± 4.2	-89.8 ± 3.9	2.6 ± 0.7
Rps. acidophila, 7050[b]	12544.1 ± 3.7	-13.1 ± 0.8	nd	12208.8 ± 6.4	-72.0 ± 6.4	-1.5 ± 0.4
Rs. molischianum, 120[b]	12584.6 ± 8.3	-28.0 ± 0.4	1.6 ± 0.1	11767.4 ± 14.5	-105.9 ± 0.6	4.6 ± 0.1
Rb. sphaeroides, 2.4.1.[c]	12511.4 ± 3.3	-27.6 ± 2.6	1.9 ± 0.5	11792.0 ± 2.2	-64.8 ± 1.7	-1.3 ± 0.3
Rb. sphaeroides, 2.4.1. WT[d]	12522.0 ± 0.9	-32.1 ± 0.6	1.8 ± 0.1	11797.0 ± 12.9	-90.3 ± 8.6	1.7 ± 1.2
Rb. sphaeroides, DPF2[d]	12517.9 ± 1.3	-27.7 ± 0.8	1.2 ± 0.1	11792.9 ± 4.5	-95.1 ± 2.9	3.6 ± 0.4
Rb. sphaeroides, B19D DD13[d]	12526.2 ± 2.5	-28.9 ± 1.9	1.3 ± 0.3	11783.1 ± 5.9	-80.2 ± 4.4	0.7 ± 0.6
Rb. sphaeroides, B19E DG2[d]	12643.4 ± 2.2	-25.6 ± 1.6	1.6 ± 0.2	11729.5 ± 6.8	-95.4 ± 5.1	2.8 ± 0.7
Rb. sphaeroides, B15 DG2[d]	12691.0 ± 3.2	-35.6 ± 2.0	1.6 ± 0.3	11749.5 ± 6.5	-93.7 ± 4.2	2.3 ± 0.5
Rb. sphaeroides, B19FDG2[d]	12817.0 ± 2.6	-42.5 ± 1.9	2.9 ± 0.3	11712.5 ± 4.9	-93.0 ± 4.0	0.7 ± 0.6

[a] The experimental dependencies have been approximated by a quadratic polynomial, $\nu = A + Sp + Cp^2$ (ν is in cm^{-1}, p is in kbar). Shown is the standard deviation of the regression parameters. [b] Detergent-isolated complexes, the actual aggregation state undetermined. [c] Isolated complexes. [d] Complexes embedded into intracytoplasmic membranes.

7050. *Rhodobacter sphaeroides* samples studied were in different integration stages. Wild type (WT) intracytoplasmic membrane vesicles (chromatophores) are intact and contain not only a full variety of light harvesting complexes (LH2, LH1), but also RC complexes. The *Rb. sphaeroides* DPF2 deletion mutant consists of LH2 antenna and RC complexes but is devoid of the core LH1 antenna complex. A series of mutants (labeled in Table 1 as B19DDD13, B19EDG2, B15DG2, and B19FDG2) includes only membrane-bound LH2 complexes containing single-site mutations at the βArg_{-10} residue (being replaced by a Met, His, Glu, and Asn residue, respectively[31]). Detergent-isolated LH2 complexes in solution complete the list of the *Rb. sphaeroides* samples.

Methods

Samples. Chromatophores and LH2 complexes were prepared according to the known procedures.[31−33] Samples were diluted with 50 mM Tris−HCl or TEN (15 mM Tris−HCl, 1 mM EDTA, 0.1 M NaCl) buffer at pH 8.0 to give a maximum absorbance in the range of 1.0−4.0 cm^{-1} (0.2−0.8 in the sample cell). Detergent-isolated samples typically contained ∼0.2% LDAO. However, our experience with the *Rb. sphaeroides* sample indicates that a somewhat higher detergent concentration is needed for maintaining LH2 complexes in a well-isolated state over a long period of time.[34] The actual aggregation state of other detergent-isolated complexes (from *Rps. acidophila* strains 10050 and 7050 and *Rs. molischianum*) has not been studied.

High-Pressure Optical Cell and Methodology of High-Pressure Spectroscopic Measurements. The homemade portable high-pressure optical cell is of the cylinder-piston type (see Figure 2). The cell is designed with three optical pathways equipped with sapphire windows. The sample solution is enclosed in a small (0.3 mL) chamber separated from the rest of the cell by two windows, ∼2 mm apart. One of these windows is fixed and the other movable in order to allow for pressure variations. The pressure in the cell is generated by a hydraulic press and transmitted to the sample volume by a glycerol−water mixture. A manganin-wire gauge is used to measure pressure in the cell and calibrate the equipment. Steady-state absorption spectra were recorded using JASCO V-530 or Beckman Acta MVII spectrophotometers, both of which were equipped with a special holder for the high-pressure optical cell.

Elastic deformation is generally believed to proceed through two more or less distinguishable kinetic steps.[35] Upon applied stress, a system undergoes an instantaneous change of interatomic distances followed by a slower structural relaxation. Therefore, our samples were allowed to equilibrate for 5−10 min after each pressure change. The pressure-induced effects were considered elastic in the considered time scale, if the data obtained along increasing and decreasing pressure routes were the same within the experimental uncertainty. Unfortunately, all antenna proteins tend to degrade to some extent with time at room temperature, even without pressurizing. Spectroscopic consequences of this "aging" include some loss of the B800 band intensity together with a red shift of the absorption and emission spectra. Isolated complexes seem to be slightly less stable compared to the membranes. Pressurizing amplifies those effects. A clear fingerprint of sample degradation is an increased intensity around 775 nm along with decreased intensity in other parts of the spectrum. Completely solubilized antenna subunits (Bchl molecules coordinated to protein polypeptides) as well as monomeric Bchl squeezed out of the proteins are known to absorb at 775 nm.[36] We tried to minimize the sample degradation by optimizing the experimental conditions to limit the measurement time. As a final measure, the increased

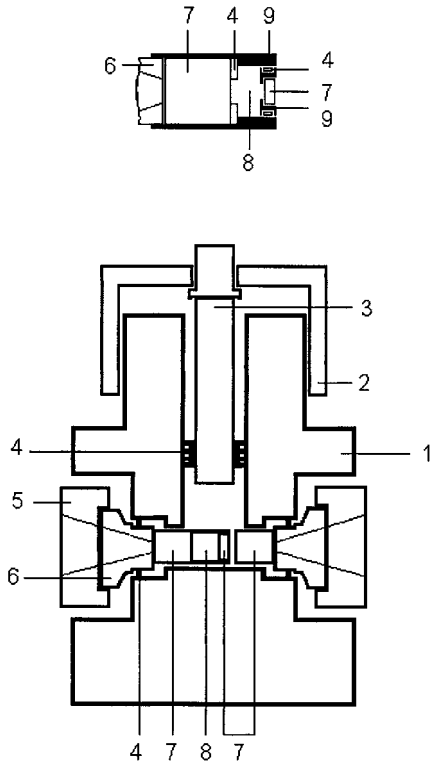

Figure 2. Schematic view of the high-pressure optical cell. For clarity, the sample cell is shown enlarged in the upper part of the figure. Key: 1, cell body; 2, fixing screw; 3, piston; 4, gasket ring; 5, screw plug; 6, window support; 7, window; 8, sample; 9, window holder.

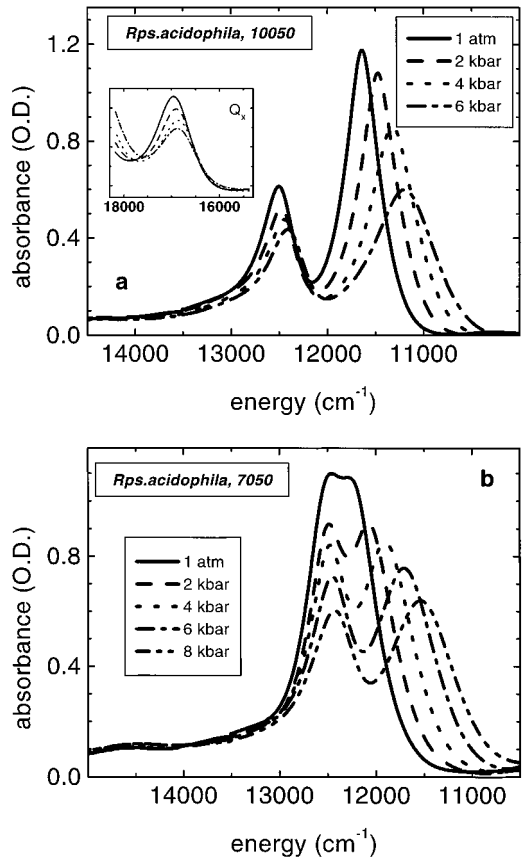

Figure 3. Effect of pressure on absorption spectra of LH2 complexes from *Rps. acidophila* (strains 10050 (a) and 7050 (b)) in the Q_y spectral range at room temperature. The legend indicates the pressure at which the spectra were recorded. The inset in part (a) depicts the Q_x region of the spectrum.

intensity around 775 nm was taken into account in the data analysis. The relatively faster degradation of the B800 absorption band suggests a partial unfolding of the *N* terminus of the ligand α-polypeptide under pressure and exposure of the binding site of the B800 molecule to the solvent phase. Whether this is a result of unfolding of the protein, of division of the LH2 into α*β*-polypeptide pairs, or of some other reason, remains to be studied.

Data Analysis. The recorded spectra were corrected for the background absorption of the high-pressure cell. The latter is determined at each pressure by measuring the absorption of the high-pressure cell without the sample, but filled in with the pressure-transmitting glycerol-water mixture. The LH2 absorption bands are asymmetric and cannot be approximated with simple Gaussians. Therefore, the absorption spectrum of mutants devoid of the B800 molecules[33] was used as a reference (with shifted origin and increased width, if necessary) to fit the B850/B820 bands. The B800 band shape is obtained as a difference between the measured spectrum of LH2 and the reference spectrum. The rest of the spectral data were analyzed using Origin 6.0 (Microcal Software, Inc.) packages.

Experimental Results

Shown in Figure 3 is the effect of applied pressure at room temperature on the Q_y absorption spectra of two LH2 complexes from *Rps. acidophila*. At ambient pressure, the absorption spectrum of the B800−850 complex (Figure 3a) consists of two well-separated bands, while that of the B800−820 complex (Figure 3b) is made of a single broad band with flattened top

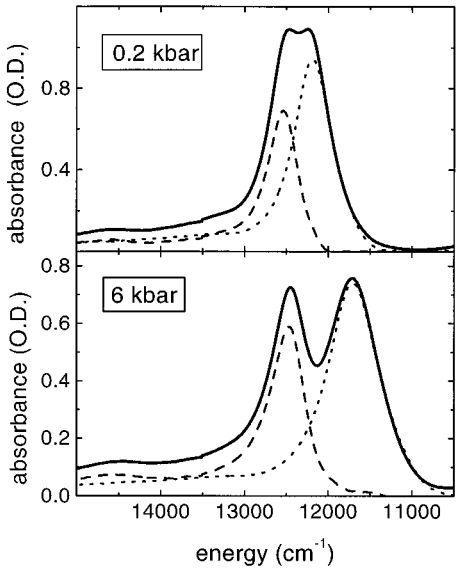

Figure 4. Room-temperature absorption spectra of the B800−820 antenna complexes from *Rps. acidophila* strain 7050 at 0.2 and 6 kbar revealing the pressure-induced split of the spectra. Shown are also the fitting subcomponents of the B800 and B820 bands.

reflecting a strong overlap of the B800 and B820 absorption bands. Both the B800 and B850/B820 bands shift to the red and broaden with increasing pressure, but with rather different rates. The B800−820 complex, revealing progressive splitting at higher pressures of the initially lone band, is a nice example of this effect. Shown in the inset of Figure 3a is a composite Q_x band that includes contributions from Bchls of both B800 and B850 rings. One can see that pressure does not lift this fortuitous energetic degeneracy at room temperature. The variations of the integrated intensity of the Q_y and Q_x absorption bands with pressure remain also within the experimental uncertainty.

The pressure dependencies of the absorption band position and bandwidth (full width at half-maximum, fwhm) were obtained as described in the Methods. The procedure is illustrated in Figure 4 for the two strongly overlapping Q_y absorption bands of the B800−820 complex. Some of the results of the band shape analysis for two samples from *Rps. acidophila* and *Rb. sphaeroides* are shown in Figure 5. The experimental dependencies were further rationalized by fitting the energy of the absorption band maximum, $\nu(p)$, and the bandwidth, $\delta(p)$, with a quadratic polynomial: $A + Sp + Cp^2$. Full account of the data in terms of the regression parameters *A* (initial value at $p = 0$), *S* (slope), and *C* (nonlinear term) is presented in Tables 1 and 2.

The most remarkable feature of the pressure-induced changes of the Q_y absorption spectra is a qualitatively different slope of the B800 and B850 band shifts. This phenomenon, first observed in ambient-temperature spectra[26] and later confirmed at low temperatures,[28] is clearly seen in Figure 6. For the sake of comparison, the curves in Figure 6 for a few different LH2 species are shifted relative to each other along the vertical axis, so that they all initiate from a single point at ambient pressure. As seen, the curves belonging to the B800 and B850/B820 bands cluster into well-separated groups irrespective of the species. It should also be noticed that the pressure-induced Q_y absorption band shift in LH1 complexes is generally larger than in LH2 complexes.

Another common feature of the pressure-induced spectral shifts is their slight (but definite, see Figures 5 and 6)

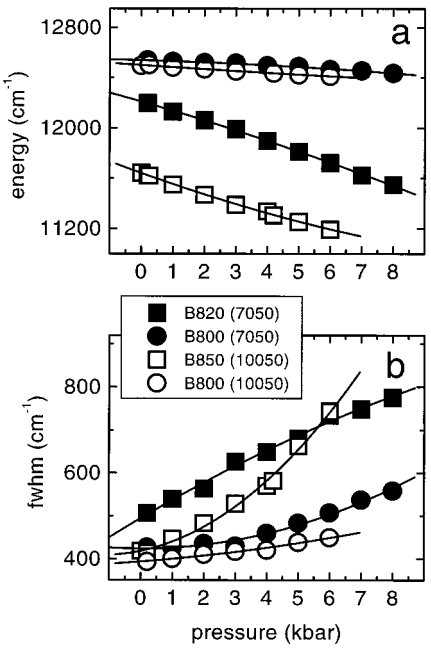

Figure 5. Effect of pressure on the position (a) and width (b) of Q_y absorption bands of B800 and B850 aggregates in two samples from *Rps. acidophila* at room temperature. Solid lines are the polynomial fits of the experimental data (dots). The regression parameters are shown in Table 1.

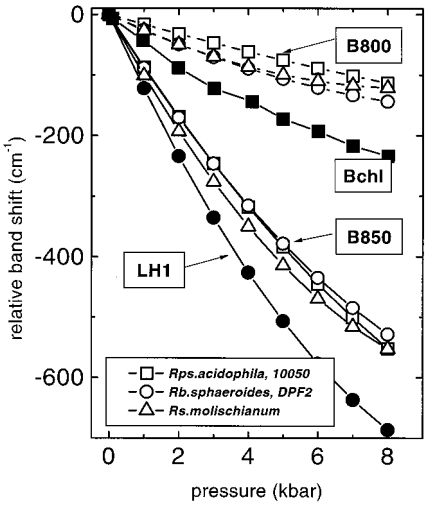

Figure 6. Relative band shifts of LH2 antennae as a function of pressure at room temperature. Straight lines are quadratic polynomials calculated using the parameters given in Table 1. For reference, data for the LH1 antenna from *Rs. rubrum*[25] and for Bchl in ether are also shown.

nonlinearity. A saturation of the speed of the pressure-induced shift of the room-temperature spectrum of *Rs. rubrum* chromatophores due to LH1 antenna complexes was earlier assigned to the decreasing compressibility of the bulk protein upon compression.[25,26] By evaluating the relative nonlinearity coefficient, *C*/*S* (where *C* and *S* are the regression parameters defined above), the nonlinear behavior of different bands can be compared. It turns out that in terms of the absolute value of *C*/*S*, the relative nonlinearity of the B800 absorption band shift is 2−3 times larger than that of the B850 band. The behaviors of the B850 band and B875 absorption band of LH1 antennas are similar. Note, however, that while the slope of the B800 band shift always decreases with pressure (which corresponds to positive sign of *C*), the sign of *C* for B850/B820 bands varies depending on antenna species (Table 1). It is thus clear that the mechanism leading to nonlinear spectral shift of strongly coupled B850/B820 and B875 bands must be more complex than considered earlier. The implication from the available data, although rather limited so far, is that *C* is negative for well-isolated and positive for membrane-embedded or otherwise aggregated antenna complexes.

A comparison of *Rps. acidophila* strain 10050 and of *Rs. molischianum* strain 120 is interesting in its own right, since the structure of the LH2 complexes in these species is known to be different. *Rps. acidophila* acquires nine and *Rs. molischianum* only eight basic units in the ring arrangement.[7,8] Moreover, the amino acid sequence of *Rs. molischianum* is partly similar to that of LH1 complexes, which is the structural basis of its altered hydrogen-bonding network compared to other LH2 complexes. At the same time, the absorption characteristics of *Rs. molischianum* recall those of regular LH2 complexes.[37] The present data support the previous observations demonstrating very similar pressure dependence of the B850 absorption bands of these two species (as well as a clear difference from the LH1 Q_y absorption band behavior (see Figure 6)). At the same time, the slope of the B800 absorption band of *Rps. acidophila* is almost 2 times smaller than that in *Rs. molischianum* suggesting a stiffer protein environment in the former (see below).

The pressure-induced shifts of the B800 and B850 Q_y absorption bands show little if any correlation with hydrogen bonds. This agrees with the idea that the compressibility of the hydrogen bonds is similar to the bulk compressibility of the proteins.[35] Two samples, most notably the B19FDG2 mutant of *Rb. sphaeroides*, show a larger slope of the B800 band shift compared to others (Table 1). As suggested in ref 24, this may be a result of a structural reorganization of the binding site of B800 Bchl molecules caused by replacement of the native Arg residue with the Asn residue.

A much too small slope of the B800 band shift for *Rb. sphaeroides* complexes was reported previously (−4.2 cm^{-1}/kbar[26]) compared to about −28 cm^{-1}/kbar found in this work (see Table 1). We favor the present data, because of clear evidence of sample degradation in the earlier work (see Figure 6 in ref 26).

We finally notice a rather strong temperature dependence of the slopes of both pressure shift and broadening of the antenna absorption spectra.[25] The corresponding slopes at low temperatures (<100 K)[25,28,30] are roughly 2 times smaller than at room temperature (refs 25 and 26 and Tables 1 and 2 of the present work). This is probably a result of the relative softness of the protein structure at physiological temperatures compared to that at low temperatures,[38] as will be discussed in some detail in one of our forthcoming papers.

Discussion

General Considerations. To begin with in Figure 7 we shall consider the origin of the singlet electronic band shifts of molecules and aggregates at ambient pressure. As shown in the left-hand side of Figure 7, electronic transition energy of a molecule in a vacuum, ν_v, is modified in a liquid or solid environment to ν_0. The energy shift, $\Delta\nu_M = \nu_0 - \nu_v$, traditionally called solvent shift, is usually (but not exclusively) toward lower energies. The physical basis of the solvent shift is that the interaction of the molecule with its surroundings is different in the electronic ground and excited states. In the aggregates composed of identical molecules (right-hand side of Figure 7), the transition energy shift relative to the unperturbed excitation energy of an aggregate can be divided into two parts. The first

TABLE 2: Pressure Dependence of the Q_y Absorption Band Widths of LH2 Antenna Complexes at Room Temperature[a]

	B800			B850/B820		
sample	A, cm^{-1}	S, cm^{-1} $kbar^{-1}$	C, cm^{-1} $kbar^{-2}$	A, cm^{-1}	S, cm^{-1} $kbar^{-1}$	C, cm^{-1} $kbar^{-2}$
Rps. acidophila, 10050[b]	393.3 ± 3.2	5.8 ± 2.5	0.6 ± 0.4	417.9 ± 6.9	15.4 ± 5.9	6.4 ± 1.0
Rps. acidophila, 7050[b]	423.5 ± 6.4	−0.2 ± 3.7	2.2 ± 0.4	493.9 ± 8.7	43.7 ± 5.1	−1.0 ± 0.6
Rs. molischianum,120[b]	393.3 ± 19.1	8.0 ± 0.8	3.0 ± 0.1	599.7 ± 7.5	19.7 ± 3.5	
Rb. sphaeroides, 2.4.1.[c]	235.8 ± 4.1	−1.4 ± 3.2	1.1 ± 0.6	332.1 ± 7.7	33.6 ± 6.1	1.7 ± 1.1
Rb. sphaeroides, DPF2[d]	406.9 ± 4.2	−13.0 ± 2.7	2.4 ± 0.3	415.8 ± 2.2	44.5 ± 1.7	1.9 ± 0.2
Rb. sphaeroides, B19D DD13[d]	407.1 ± 3.2	0.9 ± 2.4	1.7 ± 0.3	423.3 ± 2.5	52.8 ± 1.8	0.2 ± 0.3
Rb. sphaeroides, B19E DG2[d]	nd	nd	nd	496.0 ± 8.5	42.0 ± 6.3	2.0 ± 0.9
Rb. sphaeroides, B15 DG2[d]	nd	nd	nd	460.3 ± 3.7	53.8 ± 0.8	
Rb. sphaeroides, B19FDG2[d]	nd	nd	nd	438 ± 2.7	44 ± 3.7	0.2 ± 0.2

[a] The experimental fwhm are approximated by a quadratic polynomial, $\delta = A + Sp + Cp^2$ (δ is in cm^{-1}, p is in kbar). Shown is the standard deviation of the regression parameters. [b] Detergent-isolated complexes, the actual aggregation state undetermined. [c] Isolated complexes. [d] Complexes embedded into intracytoplasmic membranes; nd, not determined.

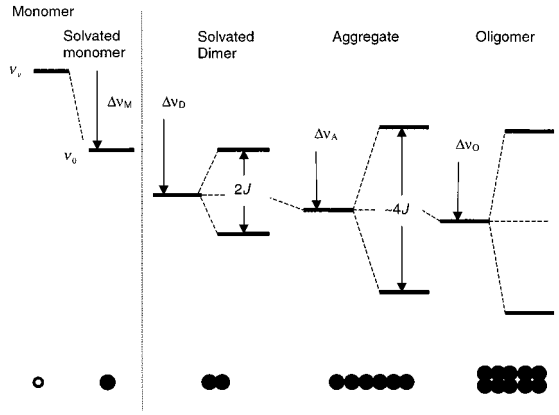

Figure 7. Schematic diagram illustrating the change of electronic transition energy of nonpolar molecules due to solvation and exciton band splitting at ambient pressure. The solvation stabilization energies due to dispersive interactions are indicated as $\Delta\nu_M$ (for a monomer), $\Delta\nu_D$ (dimer), $\Delta\nu_A$ (aggregate), $\Delta\nu_O$ (complex of aggregates or oligomer). J is the resonant coupling energy between adjacent molecules. For simplicity, the transition energies of all aggregate molecules are taken to be the same. See text for further details.

part is determined by the interactions in the system in the absence of resonant (commonly called exciton) interactions. In Figure 7, it is seen as a shift of the mean energy of the aggregate states and is denoted with $\Delta\nu_D$, $\Delta\nu_A$, $\Delta\nu_O$ for a dimer, aggregate, and oligomer, respectively. In loosely packed (i.e., without direct orbital overlap) aggregates composed of nonpolar or weakly polar molecules (like the Bchl molecule) this shift is mainly related to dispersive interactions.[2] The shift of the mean differs from the solvent shift of individual molecules, because it includes the so-called displacement term due to interactions between the molecules constituting the aggregate as well as the solvation energy difference between the aggregate and the aggregate molecules taken separately. The second part of the shift is due to exciton interactions. The latter cause delocalization of an excitation over the aggregate molecules and result in splitting of molecular terms into bands. In the particular case of a dimer, which is the simplest type of aggregate, the splitting energy equals twice the resonant coupling energy, J. In one-dimensional linear aggregates with nearest neighbor coupling the exciton bandwidth is $\sim 4J$. Compression results in translation and orientation deformations of a molecular system that changes intermolecular interactions. This in turn leads to modification of transition energies.

For a meaningful discussion of the pressure-induced changes of the antenna optical spectra, the character of the deformations of the LH2 complex caused by hydrostatic pressure needs to be known. There is a recent study of vibrational spectra of LH1 antenna complexes[29] under high hydrostatic pressure showing that at pressures similar to those used in the current work the chromophores within the protein matrix experience little if any distortion. Also, the hydrogen-bonding network involving C_2 and C_9 carbonyl groups of the chromophores remains unperturbed. This implies that at present experimental conditions not only the conformation of chromophores but also the ringlike structure of the whole LH1 complex stays intact. Similar conclusions are probably correct in the case of LH2 complexes considering a continuous red shift of absorption spectra observed in this work as well as our unpublished resonant Raman data.[39]

Expressing more generally, the above conclusion is compatible with the division of forces that maintain biological structure into "weak" and "strong" forces.[35] The limited compression achieved at present pressures (see below) is expected to modify only "weak" interactions including hydrogen bonding, electrostatic, and van der Waals interactions. "Strong" forces, such as those exerted by covalent bonds, are less relevant here, because much higher pressures are usually needed to change these bonds. This is why in the following discussion we shall assume the chromophores as virtually rigid entities, an approach that has been well tested in molecular crystal studies.[40−42]

The main effect of pressure is thus, a uniform compression of the local space accommodating chromophores in the surrounding protein. The deformations of the protein complex are considered sufficiently small, such that only linear terms in the expansion of the molecular positions and orientations as power series in the pressure need to be considered.[40−42] This affords a straightforward physical modeling, but of course, is adequate for describing the experimental results at the low-pressure limit only. The further neglect of the pressure-induced variations of the B850 chromophore orientations can be justified as follows. The angular dependence of the resonant interactions in the dipole approximation is determined by the orientation factor,[2] $\chi = \cos\alpha - 3\cos\beta\cos\eta$. Here, α is the angle between the unit vectors along the interacting transition dipoles and β and η are the angles between the unit vectors along the line joining the two dipole centers and the respective dipoles. Under hydrostatic compression one expects a conservation of those angles, at least in the low-pressure range. Closing to the steric hindrance limit may lead to angles increase. It can be shown, however, that at the given geometry of the transition dipoles in the LH2 complex[43] the angular dependence of the orientation factor is strongly suppressed. For example, a relatively large 10% increase of the angles between the projections of the antiparallel B850 transition dipoles on the circle plane and the tangent to the circle decreases the orientation factor only by ~2%.

Pressure Dependent Compressibility of the B800 Binding Site. In the case of localized molecular excitations (such as expected to be present in the B800 ring of chromophores) in homogeneous and isotropic media the dispersive interactions lead to a linear dependence of the electronic transition energy on pressure[44,45]

$$\Delta\nu(p) = 2\Delta\nu_{\mathrm{M}}(0)\kappa_T\Delta p \tag{1}$$

Here, $\kappa_T = -1/V(\partial V/\partial p)_T$ is the isothermal compressibility coefficient of the medium characterizing the ability of a system to change its bulk volume, Δp is the increment of pressure, and $\Delta\nu_{\mathrm{M}}(0)$ is the solvent shift at pressure p.

With $\Delta\nu(p)$ and $\Delta\nu_{\mathrm{M}}(0)$ known, the isothermal compressibility of the medium at ambient pressure can be estimated from eq 1. There are two guesses for the Q_y transition frequency of Bchl molecules in a vacuum: $\nu_{\mathrm{v}} \approx 13\,340$[46] and 13 590 cm^{-1}.[47] As for the reference frequency, ν_0, necessary for calculating $\Delta\nu_{\mathrm{M}}(0)$, one has to bear in mind that eq 1 is applicable only in the case of nonspecific (e.g., dispersive) solute−environment interactions. Specific interactions, such as hydrogen bonding and axial ligation, are also instrumental in tuning the antenna spectra.[21−24,37,48] A unified model considering both specific and nonspecific interactions is not yet available. However, according to ref 24, one can take ∼790 nm (12 658 cm^{-1}) as an estimate of the transition wavelength of the B800 Bchls in *Rb. sphaeroides* free from the hydrogen bonding with the surrounding protein. (This choice excludes the two last samples in Table 1 for the reason already explained in the Experimental Results.) This gives $\Delta\nu_{\mathrm{M}}(0) = -682$ or -932 cm^{-1} for the above two estimates of ν_{v} and, using the average slope from Table 1 ($\Delta\nu(p)/\Delta p \approx -28$ cm^{-1} kbar^{-1}), $\kappa_T = 0.021$ (0.015 kbar^{-1}).

Although the above compressibility concerns local mechanical properties of the binding site of the B800 molecules, the obtained number is within the typical range of bulk compressibility of globular proteins.[35,49] This averaging is probably a consequence of multiple approximations behind eq 1. Assuming homogeneous and pressure-independent compressibility, the distances within the protein decrease in average ∼0.6% per 1 kbar applied hydrostatic pressure. Equivalent volume effects can be obtained by cooling by ∼50 K (taking a linear thermal expansion coefficient of 1.15×10^{-4} K^{-1} [50]).

On the basis of eq 1, a diminishing slope of the experimental band shift with pressure can be interpreted as due to changing compressibility. A fundamental reason for the pressure dependence of the medium compressibility is the anharmonicity of intermolecular interactions.[35] Analysis of the fitting curves of the B800 band shifts in Table 1 shows that the compressibility decrease is nonlinear with pressure. Although this is in qualitative accord with the well-established functional form of the pressure dependence of the compressibility in condensed matter: $\kappa_T(p) = 1/(B_0 + B'p)$, where B_0 and B' are constants, the quantitative agreement is missing. Clearly, further studies are required for resolving this discrepancy.

Search for Evidence of Short-Range Interactions in the B850 Spectrum. In the case of delocalized excitations (as in the B850 ring), the changes of the mean of the exciton band and of the exciton interactions simultaneously contribute to the band shift under compression.[40−42] In the lowest order approximation when different shift terms are considered independent from each other, the overall slope of the exciton absorption band shift can be written as a sum of component slopes.

$$S = S_{\mathrm{D}} + S_{\mathrm{dd}} + S_{\mathrm{sr}} \tag{2}$$

where S_{D}, S_{dd}, and S_{sr} are the slopes due to dispersive, dipole−dipole, and short-range orbital overlap interactions, correspondingly. In the low-pressure limit ($p \rightarrow p_0 \simeq 0$).

$$S_{\mathrm{D}} = 2\kappa_T\Delta\nu_{\mathrm{A}}(0) \tag{3}$$

$$S_{\mathrm{R}} = -B|J_{\mathrm{dd}}(0)|\kappa_T \tag{4}$$

$$S_{\mathrm{sr}} = -\frac{2}{3}\gamma R_0|J_{\mathrm{sr}}(0)|\kappa_T \tag{5}$$

A common $\propto R^{-3}$ distance dependence of dipole−dipole couplings was assumed, while that of short-range couplings was defined as $J_{\mathrm{sr}}(R) = J_{\mathrm{sr}}(0)\exp[-\gamma(R - R_0)]$. R_0 is the distance of the closest approach between the electron donor and electron acceptor at ambient pressure, and γ is the attenuation constant. $J_{\mathrm{dd}}(0)$ and $J_{\mathrm{sr}}(0)$ are, respectively, the long-range dipolar and short-range orbital overlap coupling energies. Due to spatial heterogeneity of the mechanical properties of the protein, κ_T in eqs 3−5 may generally not be the same as in eq 1.

$\Delta\nu_{\mathrm{A}}(0)$ in eq 3 is the solvent shift of the aggregate defined as a shift of the ambient-pressure spectrum of the aggregate in the absence of exciton interactions due to a transfer of the aggregate from the vacuum to the medium. Its value, being sensitive to the immediate surroundings of the pigments (as indicated by the different mean of the B820 and B850 exciton bands) and also being generally different from the solvent shift of identical individual molecules, is not known. This appears to be one of the main difficulties in separating the experimental spectral shifts of antenna aggregates into its constituents.

To formally overcome this difficulty, we have taken the advantage of numerical simulations of aggregate exciton spectra, which show that the mean of the site energies of the two Bchl molecules coordinated to α- and β-apoproteins in B850 of *Rb. sphaeroides* is ∼12 330 cm^{-1}. This gives $\Delta\nu_{\mathrm{A}}(0) = -1010$ cm^{-1} as an upper-bound estimate relative to ν_{v}. The algorithm of the simulations is described in detail in ref 5. Similarly, a computational approach was used to estimate the coefficient B in eq 4 that depends on specific geometry of the aggregate. For the B850 aggregate of *Rb. sphaeroides* one gets $B \approx 2$ (data not shown).

The following discussion relies heavily on the B850 aggregate data of isolated LH2 complexes from *Rb. sphaeroides*, as the best characterized and most thoroughly studied sample. Assuming a uniform compressibility of the LH2 protein complex equal to 0.021 kbar^{-1}, we have $S_{\mathrm{D}} \approx -42.4$ cm^{-1}/kbar. What is left over from the measured slope $S \simeq -64.8$ cm^{-1}/kbar (Table 1) is assigned to resonant couplings. According to the ambient-pressure, ab initio molecular orbital calculations,[9] the ratio of the short-range orbital overlap and long-range dipolar coupling energies, $|J_{\mathrm{sr}}(0)|/|J_{\mathrm{dd}}(0)|$, in the B850 ring of LH2 is between 1/2 and 1/4. Taking $J(0) \approx 280$ cm^{-1} from the exciton spectral calculations[5] and $|J_{\mathrm{sr}}(0)|/|J_{\mathrm{dd}}(0)| = 1/2$, we have $J_{\mathrm{dd}}(0) \approx 187$ cm^{-1} and $J_{\mathrm{sr}}(0) \approx 93$ cm^{-1}, which leads to $S_{\mathrm{dd}} \approx -7.9$ cm^{-1}/kbar and $S_{\mathrm{sr}} \approx -14.5$ cm^{-1}/kbar.

Knowing S_{sr} and $J_{\mathrm{sr}}(0)$, it is now easy to find γ. For example, $R_0 \approx 0.35$ nm[7] gives $\gamma \approx 31.8$ nm^{-1}, which is close to the attenuation constant for electron tunneling through a vacuum, but over 2 times larger for electron transfer in typical electron-transfer proteins.[51] Within the present model framework the situation can be remedied by increasing R_0, $J_{\mathrm{sr}}(0)$ and/or κ_T. R_0 is known from the crystal structure and cannot be readily changed, unless it is defined as an effective parameter. The relative value of $J_{\mathrm{sr}}(0)$ was already chosen close to the larger limit, as suggested by theoretical calculations. At the same time,

a larger local compressibility of the surroundings of the B850/820 molecules compared to that of the B800 molecules is not only probable, but also quite likely. This is because α- and β-apoproteins are known to interact only at N- and C-termini.[7] There is no $\alpha\beta$ helix−helix contact within the transmembrane portion of the complex. As the B800 molecules are placed nearer to the surface of the protein than the B850/820 molecules, one would expect larger compressibility of the surroundings of the B850 molecules compared to the B800 binding site. A conceivable 15% increase of the compressibility to 0.024 kbar^{-1} leads to $\gamma \approx 14$ nm^{-1}, a perfectly acceptable value. Relative values of the component slopes ($S_D \approx -48.5$, $S_{dd} \approx -9.0$, and $S_{sr} \approx -7.3$ cm^{-1}/kbar) indicate that dispersive interactions give by far the largest contribution to the pressure-induced shift. The input of dipolar exciton and short-range interactions is roughly the same.

We admit that the observed slope of the B850 band shift can also be achieved within common Coulomb exciton model, without concerning short-range coupling mechanisms. Although this requires an equally reasonable ∼20% increase of the "local" B850 compressibility, a reduced or inverted curvature of the B850 absorption band shift compared to that of the B800 band (Table 1 and Figure 5) is a strong argument for the participation of short-range couplings between tightly packed chromophores in the B850 ring. This follows from eq 6 (eq 5 is a limit of eq 6 at $\Delta p \rightarrow 0$) showing that the slope S_{sr} increases with pressure.

$$S_{sr} = -\frac{2}{3}\gamma R_0 |J_{sr}(0)| \kappa_T \exp\left(\frac{1}{3}\gamma R_0 \kappa_T \Delta p\right) \qquad (6)$$

This increase may compensate and finally overcome the saturation of the spectral shift due to decreasing compressibility, which probably prevails in the case of the B800 band. In the membranes and aggregated species the effect may be masked by the larger heterogeneity of the sample.

Concluding Remarks and Summary

In the case of the B850 aggregate, the coupling between the chromophores not only causes excitation transfer along the aggregate and the corresponding exciton spectral shift but also contributes to the solvent shift. From the energy difference of the calculated mean of the exciton band and of the Q_y absorption spectrum maximum of Bchl molecules in a vacuum, this solvent shift constitutes a bigger part (approximately two-thirds) of the total B850 exciton absorption band shift at ambient pressure. As a consequence, the main contribution to the pressure dependence of the B850 band position is given by the diagonal elements of the interaction matrix, rather than by the exciton interaction terms. A more reliable division of the solvent shift into chromophore−chromophore and chromophore−protein contributions can be achieved by confronting experimental data with the results of quantum chemical calculations.

A justification for retaining in eq 2 only the dipole−dipole coupling term and not relaying on a more general point-monopole approximation, comes from ref 52. It turns out that as higher multipole contributions become significant in comparison with the dipole−dipole coupling, short-range, inter-chromophore orbital overlap interactions become much greater than the higher multipole corrections to the dipole−dipole term. In most cases, the dominant contribution to these short-range interactions arises from mixing of the locally excited donor and acceptor configurations with interchromophore charge-transfer configurations.[52]

A rough analysis of the experimental data given in the Discussion is based on analogy with classical solvent shift phenomenon. The main advantage of this approach is straightforwardness. Yet, the limitations of this model, neglect of local solvent structure and collective couplings between solute and solvent molecules, are also well-known. Moreover, interactions between the chromophores and the protein matrix are much more specific and structure-related than what is encountered in liquid solvents. Equation 1, for example, is obtained in the second-order approximation of the perturbation theory assuming random orientation of the solute-environment interactions. If these simplifying assumptions are not justified, the nonvanishing result may be obtained already in the first-order theory.[53] Clearly, further development of the theory is needed in order to use in full the potential of high-pressure spectroscopy in studying the couplings involved in precise tuning of the spectra of photosynthetic chromophore−protein complexes, and, more broadly, in environmental adaptation of photosynthetic organisms.

Summarizing the main results of the present work, it is shown that the pressure-induced shift of the B800 band is governed by pigment−protein interactions, while in addition to that, interpigment couplings (both dipole−dipole resonant and short-range exchange couplings) are instrumental for the B850 band shift. A reduction of the B800 band shift rate is observed at higher pressures, presumably due to decreasing protein compressibility. The compressibility of the B800 binding site of Bchl at ambient pressure, ∼0.02 kbar^{-1}, is within the typical range of bulk compressibility of globular proteins. The shifts show little if any correlation with hydrogen bonds.

Acknowledgment. This work was supported by the Estonian Science Foundation grant No. 3865, German-Estonian Research Project X.112.2 (BMB-WTF; IB bei der DLR) and Royal Swedish Academy of Sciences. Helpful discussions with S. H. Lin are gratefully acknowledged. We thank R. Cogdell, C. N. Hunter, B. Robert, and N. W. Woodbury for generously providing the samples and J. Herek for critical reading of the manuscript and for kindly offering the absorption spectra of the B800-less mutants. D. Leupold, H. Stiel, and M. Tars participated in the initial phase of this study.

References and Notes

(1) Förster, T. In *Modern Quantum Chemistry*; Sinanoglu, O., Ed.; Academic Press: New York, 1965; pp 93−137.
(2) Davydov, A. S. *Theory of Molecular Excitons*; Plenum Press: New York, 1971.
(3) Reddy, N. R. S.; Lyle, P. A.; Small, G. J. *Photosynth. Res.* **1992**, *31*, 167.
(4) Sauer, K.; Cogdell, R. J.; Prince, S. M.; Freer, A.; Isaacs, N. W.; Scheer, H. *Photochem. Photobiol.* **1996**, *64*, 564.
(5) Freiberg, A.; Timpmann, K.; Ruus, R.; Woodbury, N. W. *J. Phys. Chem. B* **1999**, *103*, 10032.
(6) Pullerits, T.; Chachisvilis, M.; Sundström, V. *J. Phys. Chem.* **1996**, *100*, 10787.
(7) McDermott, G.; Prince, S. M.; Freer, A. A.; Hawthornthwaite-Lawless, A. M.; Papiz, M. Z.; Cogdell, R. J.; Isaacs, N. W. *Nature* **1995**, *374*, 517.
(8) Koepke, J.; Hu, X.; Muenke, C.; Schulten, K.; Michel, H. *Structure* **1996**, *4*, 581.
(9) Scholes, G. D.; Gould, I. R.; Cogdell, R. J.; Fleming, G. R. *J. Phys. Chem. B* **1999**, *103*, 2543.
(10) Linnanto, J.; Korppi-Tommola, J. E. I.; Helenius, V. M. *J. Phys. Chem. B* **1999**, *103*, 8739.
(11) Alden, R. G.; Johnson, E.; Nagarajan, V.; Parson, W. W.; Law, C. J.; Cogdell, R. G. *J. Phys. Chem. B* **1997**, *101*, 4667.
(12) Ohigashi, H.; Shirotani, I.; Inokuchi, H.; Minomura, S. *J. Chem. Phys.* **1965**, *43*, 314.
(13) Otto, A.; Keller, R.; Rahman, A. *Chem. Phys. Lett.* **1977**, *49*, 145.
(14) Meletov, K. P.; Shchanov, M. F. *Fiz. Tverd. Tela* **1985**, *27*, 106 (in Russian).
(15) Gaidai, S. I.; Meletov, K. P. *Zhurn. Eksp. Theor. Fiz.* **1991**, *100*, 1567 (in Russian).

(16) Freiberg, A.; Allen, J. P.; Williams, J.; Woodbury, N. W. *Photosynth. Res.* **1996**, *48*, 309.
(17) Freiberg, A.; Godik, V. I.; Pullerits, T.; Timpmann, K. E. *Chem. Phys.* **1988**, *128*, 227.
(18) Freiberg, A.; Godik, V. I.; Pullerits, T.; Timpman, K. *Biochim. Biophys. Acta* **1989**, *973*, 93.
(19) Pullerits, T.; Sundström, V. *Acc. Chem. Res.* **1996**, *29*, 381.
(20) Hayashi, H.; Nozawa, T.; Hatano, M.; Morita, S. *J. Biochem.* **1981**, *89*, 1853.
(21) Sturgis, J. N.; Jirsakova, V.; Reiss-Husson, F.; Cogdell, R. J.; Robert, B. *Biochemistry* **1995**, *34*, 517.
(22) Sturgis, J. N.; Robert, B. *J. Phys. Chem. B* **1997**, *101*, 7227.
(23) Fowler, G. J. S.; Sockalingum, G. D.; Robert, B.; Hunter, C. N. *Biochem. J.* **1994**, *299*, 695.
(24) Gall, A.; Fowler, G. J. S.; Hunter, C. N.; Robert, B. *Biochemistry* **1997**, *36*, 16282.
(25) Freiberg, A.; Ellervee, A.; Kukk, P.; Laisaar, A.; Tars, M.; Timpmann, K. *Chem. Phys. Lett.* **1993**, *214*, 10.
(26) Tars, M.; Ellervee, A.; Kukk, P.; Laisaar, A.; Saarnak, A.; Freiberg, A. *Lithuanian J. Phys.* **1994**, *34*, 320.
(27) Wu, H.-M.; Savikhin, S.; Reddy, N. R. S.; Jankowiak, R.; Cogdell, R. J.; Struve, W. S.; Small, G. J. *J. Phys. Chem.* **1996**, *100*, 12022.
(28) Wu, H.-M.; Ratsep, M.; Jankowiak, R.; Cogdell, R. J.; Small, G. J. *J. Phys. Chem. B* **1997**, *101*, 7641.
(29) Sturgis, J. N.; Gall, A.; Ellervee, A.; Freiberg, A.; Robert, B. *Biochemistry* **1998**, *37*, 14875.
(30) Reddy, N. R. S.; Wu, H.-M.; Jankowiak, R.; Picorel, R.; Cogdell, R. J.; Small, G. J. *Photosynth. Res.* **1996**, *48*, 277.
(31) Fowler, G. J. S.; Hess, S.; Pullerits, T.; Sundström, V.; Hunter, C. N. *Biochemistry* **1997**, *36*, 11282.
(32) Cogdell, R. J.; Hawthornthwaite, A. M. In *Photosynthetic Reaction Centers*; Deisenhofer, J. N., James, R., Eds.; Academic Press: San Diego, 1993; pp 23−42.
(33) Herek, J. L.; Fraser, N. J.; Pullerits, T.; Martinsson, P.; Polivka, T.; Scheer, H.; Cogdell, R. J.; Sundström, V. *Biophys. J.* **2000**, *78*, 2716.
(34) Timpmann, K.; Woodbury, W. N.; Freiberg, A. *J. Phys. Chem. B* **2000**, *104*, 9769.
(35) Kharakoz, D. P. *Biophys. J.* **2000**, *79*, 511.
(36) Loach, P. A.; Parkes-Loach, P. S. In *Anoxygenic Photosynthetic Bacteria*; Blankenship, R. E., Madigan, M. T., Bauer, C. E., Eds.; Kluwer Academic Publishers: Dordrecht, The Netherlands, 1995; pp 437−471.
(37) Visschers, R. W.; Germeroth, L.; Michel, H.; Monshouwer, R.; van Grondelle, R. *Biochim. Biophys. Acta* **1995**, *1230*, 147.
(38) Zaccai, G. *Science* **2000**, *288*, 1604.
(39) Gall, A. Personal communication.
(40) Sugakov, V. I. In *Excitons*; Rashba, E. I., Sturge, M. D., Eds.; North-Holland: Amsterdam, 1982; pp 711−733.
(41) Rice, S. A.; Jortner, J. In *Physics of Solids at High Pressures*; Tomizuka, C. T., Emric, R. M., Eds.; Academic Press: New York, 1965; pp 63−168.
(42) Schipper, P. E. *Mol. Cryst. Liq. Cryst.* **1974**, *28*, 401.
(43) Freer, A.; Prince, S.; Sauer, K.; Papiz, M.; Hawthornthwaite-Lawless, A.; McDermott, G.; Cogdell, R.; Isaacs, N. W. *Structure (London)* **1996**, *4*, 449.
(44) Sesselmann, T.; Richter, W.; Haarer; Morawitz, H. *Phys. Rev. B* **1987**, *36*, 7601.
(45) Laird, B. B.; Skinner, J. L. *J. Chem. Phys.* **1989**, *90*, 3274.
(46) Renge, I. *Chem. Phys.* **1992**, *167*, 173.
(47) Limantara, L.; Sakamoto, S.; Koyama, Y.; Nagea, H. *Photochem. Photobiol.* **1997**, *65*, 30.
(48) Fowler, G. J. S.; Visschers, R. W.; Grief, G. G.; Van Grondelle, R.; Hunter, C. N. *Nature* **1992**, *355*, 848.
(49) Gekko, K.; Hasegawa, Y. *Biochemistry* **1986**, *25*, 6563.
(50) Frauenfelder, H.; Hartmann, H.; Karplus, M.; Kuntz, I. D.; Kuriyan, J.; Parak, F.; Petsko, G. A.; Ringe, D.; Tilton, R. F.; Connolly, M. L.; Nelson, M. *Biochemistry* **1987**, *26*, 254.
(51) Arnaut, L. G.; Formosinho, S. J. *J. Photochem. Photobiol. A: Chemistry* **1996**, *100*, 15.
(52) Scholes, G. D.; Fleming, G. R. *J. Phys. Chem. B* **2000**, *104*, 1854.
(53) Lin, S. H. Personal communication.